BNAM 2018
Baltic-Nordic Acoustics Meeting
15-18 April 2018
Harpa, Reykjavík, Iceland

Efficient sound barrier calculations with the BEM

Peter Møller Juhl
The Mads Clausen Institute, University of Southern Denmark
Campusvej 55, DK-5230 Odense M, Denmark, pmjuhl@mci.sdu.dk

Vicente Cutanda Henríquez
DTU Electrical Engineering, Technical University of Denmark
Ørsteds Plads Building 352, DK-2800 Kgs. Lyngby, Denmark, vcuhe@elektro.dtu.dk

The Boundary Element Method has been used for calculating the effect of introducing sound barriers for some decades. The method has also been used for optimizing the shape of the barrier and in some cases the effects of introducing sound absorption. However, numerical calculations are still quite time consuming and inconvenient to use, which is limiting their use for many practical problems. Moreover, measurements are mostly taken in one-third or full octave bands opposed to the numerical computations at specific frequencies, which then has to be conducted using a fine density in frequencies. This paper addresses some of the challenges and possible solutions for developing BEM into a more efficient tool for sound barrier calculations.

1 Introduction

Today, calculations using the Boundary Element Method (BEM) can more or less routinely be performed for predicting the insertion loss of noise barriers. The BEM is able to handle homogeneous conditions in air (e.g. no refraction due to wind or temperature gradients) and in the ground (e.g. rigid ground or locally reacting ground given by an impedance model). An open-source software tool such as OpenBEM [1] has been downloaded a large number of times by users searching for a tool for insertion loss prediction/sound barrier optimization, but the BEM is still too cumbersome to use - both in terms of ease-of-use and calculation time – in order to be in everyday use by e.g. engineers and road noise authorities.

Ease-of-use has been addressed by improving the interface to the OpenBEM code. Standard barrier shapes based on parametric input (such as height and width of the barrier) are introduced allowing fast and convenient set-up of popular barrier shapes. However, the user can still deal with general barrier shapes using the previous interface. The improvements with respect to ease-of-use are not discussed further in the present paper – it is more conveniently explored by trying out the code.

Calculation time remains an issue because barrier calculations are relevant in a large frequency range, at low frequencies the barrier is typically smaller or comparable to wavelength, whereas at high frequencies, the barrier is large compared to the wavelength. At medium and high frequencies many elements must therefore be used in order to resolve the acoustic field (as a rule of thumb 5-6 nodes per wavelength are needed) leading to significant computational work. In the upper range of frequencies ray-based models can often be employed for predicting barrier efficiency. Another issue that also tend to increase computational work is the fact that for many source-barrier-receiver configurations interference plays an important role: depending on the configuration sharp dips can occur in calculated curves over insertion loss as a function of frequency. The exact position of these narrow-band dips will depend strongly on the exact positions of the source and receiver and of the speed of sound used in the calculations. In contrast to this, measurements are often carried out in, say, one-third octave bands smoothening out the response. In order to average calculated

responses in frequency bands, a high frequency resolution is needed – in particular at high frequencies, where the response can vary significantly with frequency. The efficient calculation of insertion losses at many frequencies is the primary concern in the present paper.

2 The 2D BEM for outdoor sound propagation above homogeneous ground

For calculating the insertion loss and similar quantities of noise barriers a 2-D method is often employed. Besides the reduction in computational work, the sound source (e.g. a 'stream' of cars or a train) is often as well represented with a line source as with a number of point sources. Furthermore, it has been established that if the barrier is not too short, insertion losses calculated using a 2-D model approximate results found using full 3-D models well [2]. Therefore consider a two-dimensional domain *V* above a plane ground surface *P*, and outside a barrier defined by its generator *L* as sketched in Figure 1. Omitting the time factor $e^{-i\omega t}$, the complex sound pressure amplitude $\hat{p}$ is the solution of the 2-D Helmholtz equation

$$\frac{\partial^2 \hat{p}(x,y)}{\partial x^2} + \frac{\partial^2 \hat{p}(x,y)}{\partial y^2} + k^2 \hat{p}(x,y) = 0. \tag{1}$$

Defining the Greens function $G(\mathbf{r},\mathbf{r}_0)$ as the solution to

.

$$\frac{\partial^2 G(\mathbf{r},\mathbf{r_0})}{\partial x^2} + \frac{\partial^2 G(\mathbf{r},\mathbf{r_0})}{\partial y^2} + k^2 G(\mathbf{r},\mathbf{r_0}) = \delta(\mathbf{r}-\mathbf{r_0}), \tag{2}$$

leads to [3]

$$G(\mathbf{r},\mathbf{r_0}) = -\frac{\mathrm{i}}{4}\mathrm{H}_0^{(1)}(kR) - \frac{\mathrm{i}}{4}\mathrm{H}_0^{(1)}(kR') + P_\beta(kR'), \tag{3}$$

where *R* is the distance between $\mathbf{r}_0$ and $\mathbf{r}$ and *R'* is the distance between the mirror source $\mathbf{r}'_0$ and $\mathbf{r}$. If the domain in question is free space, only the first term in Equation (3) appear, whereas the first two terms appear for propagation above a rigid plane. The third term in Equation (3) arises for propagation above a homogeneous ground characterized by the normalized admittance β:

$$P_\beta(kR') = \frac{\beta \mathrm{e}^{ikR'}}{\pi}\int_0^\infty t^{-\frac{1}{2}}\mathrm{e}^{-kR'}g(t)\mathrm{d}t + \frac{\beta \mathrm{e}^{\mathrm{i}kR'(1-a_+)}}{2\sqrt{(1-\beta^2)}}\mathrm{erfc}\left(\mathrm{e}^{-\frac{\mathrm{i}\pi}{4}}\sqrt{kR'}\sqrt{a_+}\right). \tag{4}$$

For definition of a+ and g(t) the reader is referred to Reference [3], where a detailed discussion of Equation (4), its limiting cases and its implementation can be found.

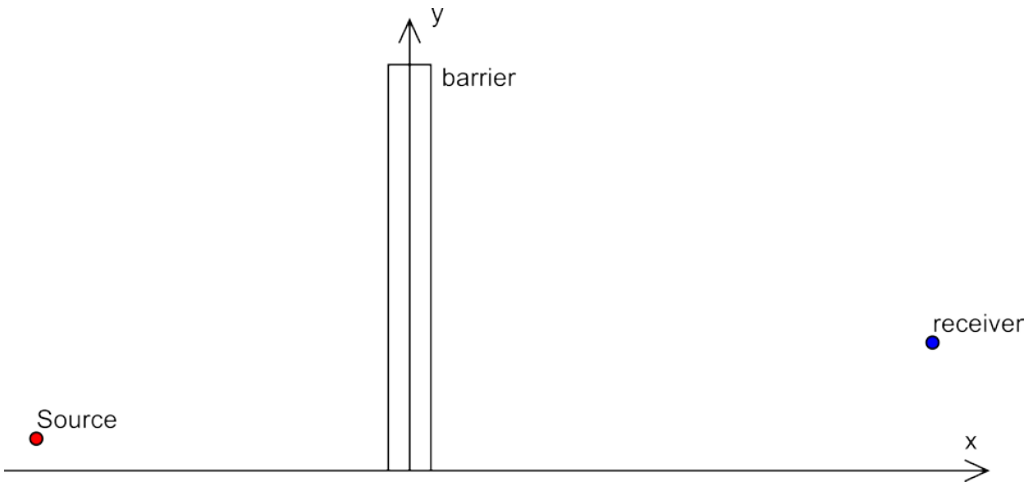

Figure 1: A barrier above a rigid or absorbing ground defined at y=0. Source and receiver positions are indicated

Since the plane is worked into the Green's function, the corresponding integral equation becomes

$$C(\mathbf{r})\hat{p}(\mathbf{r}) = \hat{p}_{inc}(r) + \int_L -\hat{p}(\boldsymbol{r_0})\frac{\partial G(\mathbf{r},\mathbf{r_0})}{\partial \mathbf{n}} + G(\mathbf{r},\mathbf{r}_0)\frac{\partial \hat{p}(\boldsymbol{r_0})}{\partial \mathbf{n}}\,\mathrm{d}L, \tag{5}$$

in which $\hat{p}_{inc}$ is the incoming field and $C(\mathbf{r})$ is a geometrical constant [1]. By standard collocation Equation (5) results in a matrix equation:

$$\mathbf{A_{tot}p} = \mathrm{i}k\rho c\mathbf{B}_{\boldsymbol{tot}}\mathbf{v}_\mathrm{n} + \mathbf{p}_{inc}\ , \tag{6}$$

where Eulers equation has been used to relate the normal derivative of the pressure to the normal velocity $\mathbf{v}_\mathrm{n}$. The matrices in Equation (6) are defined as

$$\mathbf{A_{tot}} = \mathbf{C} + \langle\int_{L_j} N_j \frac{\partial}{\partial n}(\tfrac{\mathrm{i}}{4}\mathrm{H}_0^{(1)}(kR))\mathrm{d}L_j\rangle_{i,j} + \langle\int_{L_j} N_j \frac{\partial}{\partial n}(\tfrac{\mathrm{i}}{4}\mathrm{H}_0^{(1)}(kR') - P_\beta(kR'))\mathrm{d}L_j\rangle_{i,j} = \mathbf{C}+\mathbf{A}+\mathbf{A'} \tag{7a}$$

$$\mathbf{B_{tot}} = -\langle\int_{L_j} N_j(\tfrac{\mathrm{i}}{4}\mathrm{H}_0^{(1)}(kR))\mathrm{d}L_j\rangle_{i,j} - \langle\int_{L_j} N_j\left(\tfrac{\mathrm{i}}{4}\mathrm{H}_0^{(1)}(kR') + P_\beta(kR')\right)\mathrm{d}L_j\rangle_{i,j} = \mathbf{B}+\mathbf{B'} \tag{7b}$$

in which the $<*>_{\mathrm{i,j}}$ notations refers to kernel-integrals over element L_j with respect to collocation point i, and N_j denotes the shape-functions used in discretizing the pressure and normal velocity respectively – please refer to References [1,6] for further details. The framework above can also be used to handle barriers with absorbing faces – if a normalized admittance $\mathbf{Y}_\mathrm{b}$ is defined along the generator of the barrier, Equations (6) becomes

$$(\mathbf{A_{tot}}+\mathrm{ik}\mathbf{B_{tot}}\mathbf{Y_b})\mathbf{p} = \mathrm{i}k\rho c\mathbf{B_{tot}}\mathbf{v}_\mathrm{n} + \mathbf{p}_{inc}\ , \tag{8}$$

in which $\mathbf{Y}_\mathrm{b}$ will contain values on the diagonal only if the surface is locally reacting. Once the pressure on the surface of the barrier has been calculated, the pressure elsewhere in the domain can be calculated directly by a discretized version of equation (5) – if only few domain points are needed, this post-processing takes insignificant time and storage.

2.1 Frequency interpolation

Equation (8) can readily be used to calculate the performance of barriers, the influence of their shape and the effect of introducing absorbing materials on barriers. However, one should be aware that BEM calculations are at specific frequencies, whereas measurements are often conducted in frequency bands – say one-third octave bands. In many cases the effect of the barrier depends strongly with the position of the source and the receiver, and the resulting insertion loss can often vary strongly with frequency due to interference effects. Therefore, calculations at many frequencies are often required. In the 2-D BEM, it is often the setting-up of equations (e.g. the numerical calculations of Equations (7) rather than the matrix solution of Equation (8) that is the time consuming part, and interpolation of the elements in the matrices could potentially save a significant amount of time. However, since $H_0^{(1)}(kR)$ varies as $\mathrm{e}^{\mathrm{i}kR}/\sqrt{kR}$ for large arguments, it is not well suited for interpolation in frequencies due to its fast variation with frequency for large distances, which is inevitable when dealing with barriers, that are large compared to the wavelength. Therefore, frequency interpolation depends on a scaling, that can compensate for the fast variation of the elements in the matrices [4,5].

Each of the elements in A and B consists of integrals of a piece of the generator L with respect to the collocation point in such a way that the element $\mathrm{a_{ij}}$ in equation (7a) consist of an integral over the element, that contain node number j with respect to collocation point number i. The distance R between nodes i and j may be large which is what leads to fast variation of the integrand, even though the length of the element is only a fraction of the wavelength. The idea is now to scale each element in **A** with a factor of $\exp(-\mathrm{i}kR_{ij})$ so that the complex exponentials become $\exp(\mathrm{i}k(R-R_{ij}))$, which will have a slow variation with respect to k (and thereby the frequency), since R-R_{ij} is small compared to the wavelength. When introducing a reflecting barrier the situation is slightly more involved compared to the cases presented in References [4] and [5], since the last terms in Equations (7) involve scaling with respect to the mirror of L, and thereby leading to a scaling factor of $\exp(\mathrm{i}kR'_{ij})$. Therefore, both **A** and **B** must be divided into two parts **A**, **A'** and **B**, **B'** respectively before scaling and interpolation in order to account for their dependence on kR and kR' respectively.

Let $\mathbf{ER}_\mathrm{k}$ denote the M by M symmetric matrix (M being the number of nodes in the BEM model) with entries $\mathrm{er}_{ij} = \exp(-\mathrm{i}kR_{ij})$ and let $\mathbf{ER'}_\mathrm{k}$ denote the corresponding matrix with entries $\mathrm{er'}_{ij}=\exp(-\mathrm{i}kR'_{ij})$. Denoting the Hadamard product (the elementwise product) of two matrices **A** and **B** by $\mathbf{A}\circ\mathbf{B}$, the scaled versions of matrices A and B become

$$\mathbf{A}_{sc,k} = \mathbf{A}_{\boldsymbol{k}} \circ \mathbf{ER}_{\boldsymbol{k}},\ \ \mathbf{A_{sc,k}}' = \mathbf{A}'_{\boldsymbol{k}} \circ \mathbf{ER}'_{\boldsymbol{k}}\ ,\ \mathbf{B}_{sc,k} = \mathbf{B}_{\boldsymbol{k}} \circ \mathbf{ER}_{\mathbf{k}} \text{ and } \mathbf{B'_{sc,k}} = \mathbf{B_k}' \circ \mathbf{ER_k}', \tag{9}$$

where index k refers to the wavenumber used when scaling. The scaled matrices are well suited for interpolation with respect to k (frequency) a linear interpolation of **A** between frequencies k_1 and k_2 would consist of scaling, interpolation and de-scaling:

$$\mathbf{A_{tot,k}} = \left(\frac{k_2 - k}{k_2 - k_1}\,\mathbf{A_{sc,k_1}} + \frac{k - k_1}{k_2 - k_1}\,\mathbf{A_{sc,k_2}}\right) \circ conj(\mathbf{ER_k}) + \left(\frac{k_2 - k}{k_2 - k_1}\,\mathbf{A'_{sc,k_1}} + \frac{k - k_1}{k_2 - k_1}\,\mathbf{A'_{sc,k_2}}\right) \circ conj(\mathbf{ER'_k}), \qquad (10)$$

where conj($\mathbf{ER}_k$) denote the complex conjugate of $\mathbf{ER}_k$, and is used to de-scale the matrices after interpolation in order to re-introduce the fast variation with frequency.

If a quadratic interpolation scheme is desired between frequencies corresponding to k_1, k_2 and k_3, the corresponding interpolation functions would be

$$K_1 = \frac{k_2 - k}{k_2 - k_1}\frac{k_3 - k}{k_3 - k_1};\; K_2 = \frac{k - k_1}{k_2 - k_1}\frac{k_3 - k}{k_3 - k_2};\; K_3 = \frac{k - k_1}{k_3 - k_1}\frac{k - k_2}{k_3 - k_2}. \qquad (11)$$

3 Calculation results and efficiency

The initial calculations concern a test case with a barrier on a rigid plane. The height of the barrier is 3 m. and its width is 0.1 m. In order to remove interference from ground reflections, both the source and the receiver are placed on the ground: the source is at (-5,0) m. and the receiver is placed at (30,0) m.; the barrier is placed at origo - see Figure 1. The barrier is modelled using 119 quadratic elements (239 nodes) and the time used for setting up the system of equations is 5-6 s. per frequency on a regular PC. The time needed to solve the system of equations is negligible (by comparison). The quantity shown in Figure 2 is the insertion loss of the barrier, defined as the ratio of sound pressure amplitudes at the receiver point with and without the barrier (but including the ground).

$$IL = 20 * \log_{10}(|\hat{p}_{barrier}(\mathbf{r}_{rec})|/|\hat{p}_{inc}(\mathbf{r}_{rec})|) \quad . \qquad (12)$$

From Figure 2 it is evident that the interpolation is very successful: even if only every 11th frequency is explicitly calculated (interpolating the matrices at 10 frequencies between those frequencies), the results agree very well. Hence, the increase in calculation speed is more than ten-fold with no significant loss in accuracy.

In the next test case the source and receiver is elevated from the ground so that the source is at (-5, 0.3) m. and the receiver at (30, 1.2) m. Several strong interference dip occurs between 500 and 800 Hz. However, the insertion loss is well predicted even with a large stepping between explicitly calculated matrices, even though some inaccuracy can be seen using the large stepping in the range of frequencies where the dip occur.

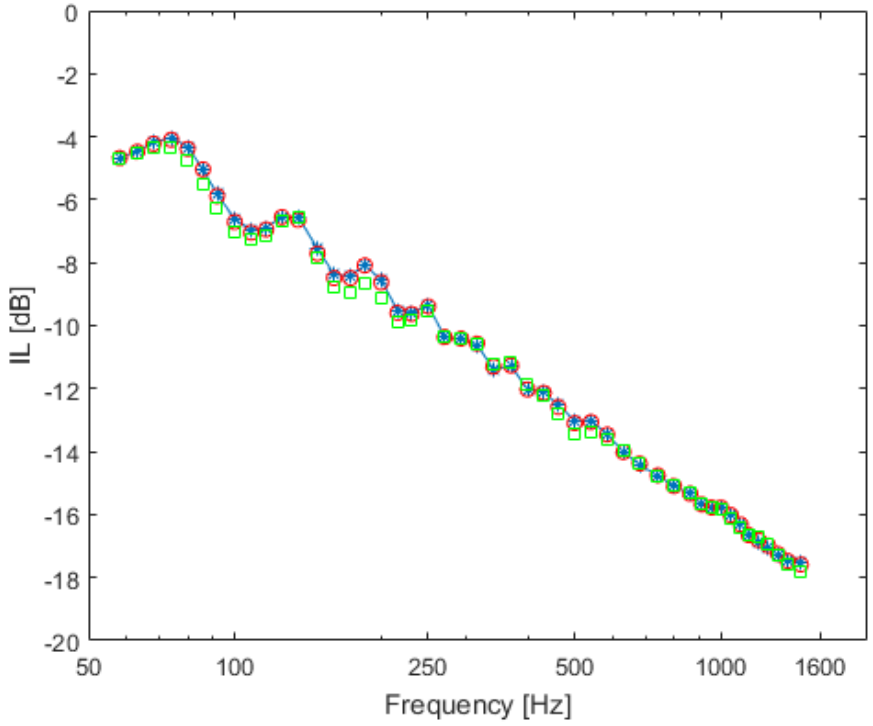

Figure 2: Insertion loss as a function of frequency for a 3 m. straight barrier. Source at (-5,0) m. and receiver at (30,0) m. -*-: calculations at every frequency; O: calculation at every fifth frequency and matric interpolation in between; □: calculation at every 11th frequency and matrix interpolation in between.

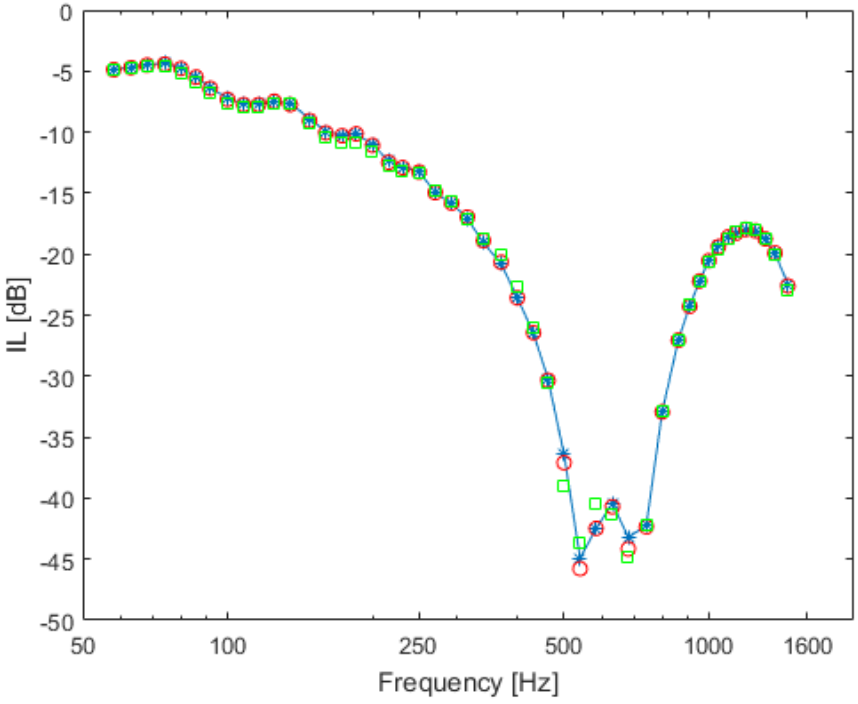

Figure 3: Insertion loss as a function of frequency for a 3 m. straight barrier. Source at (-5,0.3) m. and receiver at (30,1.2) m. -*-: calculations at every frequency; O: calculation at every fifth frequency and matric interpolation in between; □: calculation at every 11th frequency and matrix interpolation in between.

4 Summary

A frequency interpolation scheme has been adapted for 2-D BEM calculations for barriers and other objects placed on a rigid or absorbing plane. Before the interpolation, the BEM matrices are scaled in order to neutralize the fast variation with frequency due to the oscillating integrands in the kernels. The interpolated matrices are then re-scaled before the calculation is carried out at the frequency desired. Using this scaling method, a significant computational work can be saved with only minor loss in accuracy. The main drawback of the presented method is the cost of computer memory, due to the need of assessing several matrices at a time. However, this issue did not become a limitation for the two dimensional cases studied here. The proposed scheme can easily be adapted to parallel processing, which will speed up calculations even further.

References

[1] V. Cutanda Henríquez and P.M. Juhl, *OpenBEM – An Open Source Boundary Element Method Software in Acoustics*. Proceedings Internoise 2010, CD-ROM, 2010

[2] D. Duhamel, *Efficient Calculation of the Three-Dimensional Sound Pressure Field around a Noise Barrier*, Journal of Sound and Vibration **197**(5), 547-571, 1996

[3] S.N. Chandler-Wilde and D.C. Hothersall, *Sound Propagation above an Inhomogeneous Impedance Plane*, Journal of Sound and Vibration **98**(4), 475-491, 1985

[4] G.W. Benthien and H.A. Schenck, *Structural-Acoustic Coupling*, Boundary Element Methods in Acoustics (Editors: R.D. Ciskowski and C.A. Brebbia), 1991

[5] P. Juhl, V. Cutanda Henríquez and D. Vanderelst, *Calculation of Head Related Transfer Functions of bats using the Boundary Element Method*, Proceedings NAG/DAGA 2009, CD-ROM, 2009

[6] P.M. Juhl, *The Boundary Element Method for Sound Field Calculations*, Report no.55/PhD dissertation, The Acoustics Laboratory, Technical University of Denmark, 1993